Structure and magnetism of Ge_3Mn_5 clusters

A. Jain,[1] M. Jamet,[1,a)] A. Barski,[1] T. Devillers,[1] I.-S. Yu,[1] C. Porret,[1] P. Bayle-Guillemaud,[1] V. Favre-Nicolin,[1] S. Gambarelli,[2] V. Maurel,[2] G. Desfonds,[2] J. F. Jacquot,[2] and S. Tardif[3]

[1]*Institut Nanosciences et Cryogénie, SP2M, CEA-UJF, F-38054 Grenoble, France*
[2]*Institut Nanosciences et Cryogénie, SCIB, CEA-UJF, F-38054 Grenoble, France*
[3]*Insitut Néel, CNRS-UJF, F-38054 Grenoble, France*

(Received 28 September 2010; accepted 23 November 2010; published online 10 January 2011)

We have grown Ge_3Mn_5 clusters by codepositing germanium and manganese atoms on Ge(001) substrates using low temperature molecular beam epitaxy and further annealing the films at high temperature. Clusters are spherical and randomly distributed in the germanium film in epitaxial relationship with the diamond lattice. They exhibit a broad size distribution. By performing a careful x-ray diffraction analysis, we could find that 97% of Ge_3Mn_5 clusters have their *c*-axis perpendicular to the film plane while 3% exhibit in-plane *c*-axis. We could also show a slight in-plane distortion of the Ge_3Mn_5 lattice leading to a reduction of uniaxial magnetic anisotropy. These observations are well confirmed by complementary superconducting quantum interference device and electron paramagnetic resonance measurements. *© 2011 American Institute of Physics*. [doi:10.1063/1.3531222]

I. INTRODUCTION

Research on ferromagnetic semiconductors (FMSs) has been evolving very fast for their potential use in spintronics. Indeed predicted electrical control of magnetism as well as high carrier spin polarization make FMS very attractive.[1] Up to now, efforts have mainly focused on diluted magnetic semiconductors (DMSs) in which magnetic atoms substitute the host matrix atoms. The most spectacular achievement was Mn-doped GaAs which has become a model system combining ferromagnetic and semiconducting properties.[2] However Curie temperatures in these materials still remain quite modest. One possible way to work at higher temperatures is to use condensed magnetic semiconductors[3] in which Mn-rich precipitates or secondary phase nanostructures form during sample growth or annealing.[4–6] Indeed Mn-rich precipitates and secondary phase crystallites usually exhibit much higher Curie temperatures than DMS. Moreover hybrid ferromagnet/semiconductor may exhibit original magnetic and transport properties that could be used in future spintronic devices.[7] Germanium or silicon based condensed semiconductors are among the most interesting for their compatibility with mainstream silicon technology. In particular, during the growth or annealing of (Ge,Mn) thin films, there is tendency to form thermodynamically favorable ferromagnetic precipitates of Ge_3Mn_5.[8–11] In order to use these ferromagnetic precipitates in complex vertical heterostructures for spintronics, one has to control their nucleation, size, and magnetic properties. In this present paper, we have investigated the structure and magnetic properties of Ge_3Mn_5 clusters obtained by annealing (Ge,Mn) films and correlated the results from various measurement techniques.

a)Electronic mail: matthieu.jamet@cea.fr.

II. EXPERIMENTAL TECHNIQUES

$Ge_{1-x}Mn_x$ thin films were grown by low temperature molecular beam epitaxy on epiready Ge(001) substrate. The growth process is explained in detail in Ref. 12. The growth of (Ge,Mn) films at high temperature (>180 °C) or annealing (Ge,Mn) films grown at low temperature above 600 °C for 15 min leads to the formation of randomly distributed spherical Ge_3Mn_5 clusters.

The crystalline structure and morphology of these films have been investigated by transmission electron microscopy (TEM) and x-ray diffraction (XRD). The TEM observations were performed using a JEOL 4000EX microscope with an acceleration voltage of 400 kV. Superconducting quantum interference device (SQUID) and electron paramagnetic resonance (EPR) techniques were used to study the magnetic properties and hence calculate the anisotropy constant of Ge_3Mn_5 clusters. For its high sensitivity and field resolution, EPR is a powerful tool to investigate anisotropy of (Ge,Mn) nanostructures.[13,14] EPR experiments were performed at $T=5$ K using a Bruker ESP 300 spectrometer. The spectrometer was operating at X-band (9.4 GHz) with a modulation frequency of 100 kHz and a modulation amplitude of 10 Oe for lock-in detection. The measurements were performed in the out-of-plane configuration with the static field $\mu_0\vec{H}$ applied from $[00\bar{1}]$ to [001] crystal direction.

III. STRUCTURE OF GE_3MN_5 CLUSTERS

In this paper, Ge_3Mn_5 clusters were obtained by annealing (Ge,Mn) films grown at low temperature at 600 °C for 15 min. The reflection high-energy electron diffraction pattern of annealed samples is exactly the same as that of Ge as clusters are away from the surface, also verified in high resolution TEM (HRTEM) image [Fig. 1(a)]. Chemical analysis at the nanometer scale using electron energy loss spectroscopy (EELS) clearly shows Ge_3Mn_5 clusters as Mn-rich re-

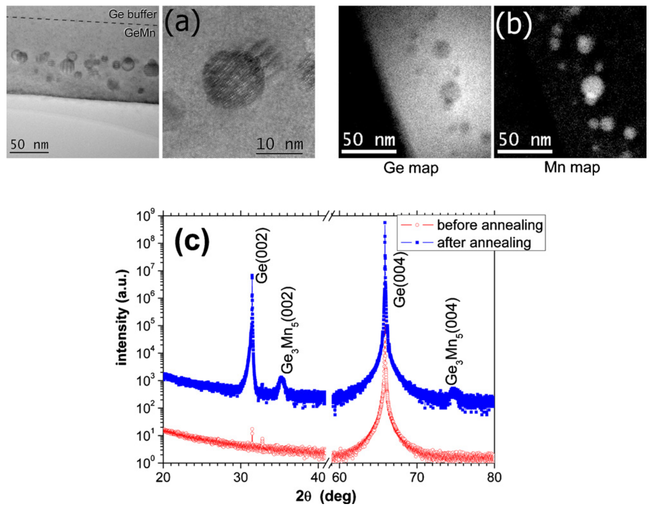

FIG. 1. (Color online) (a) HRTEM image of a $Ge_{0.94}Mn_{0.06}$ thin film grown at 130 °C and annealed at 650 °C for 15 min. Spherical Ge_3Mn_5 clusters are clearly visible. (b) Energy filtered TEM images using EELS and showing Ge and Mn rich zones and (c) $\theta/2\theta$ XRD spectra of a $Ge_{0.94}Mn_{0.06}$ film grown at 130 °C before and after annealing at 650 °C for 15 min.

gions whereas Mn concentration in the surrounding Ge matrix is within the resolution limit of this technique [Fig. 1(b)]. Finally XRD measurements in $\theta/2\theta$ mode further suggest that these Ge_3Mn_5 clusters have their c-axis [001] lying along the Ge [001] direction [Fig. 1(c)]. In order to verify the different orientations of clusters, we performed grazing incidence XRD at $\lambda=0.120\,37$ nm, searching for all possible Ge_3Mn_5 reflections in the plane parallel to the sample surface. Measurements were performed at the European Synchrotron Radiation Facility (ESRF, Grenoble, France). The incident angle (0.3°) was chosen by maximizing the scattered intensity from the buried clusters. As is shown in Fig. 2, only two possible configurations are possible for the clusters:

(1) c-axis perpendicular to the sample surface [along $(001)_{Ge}$] and a-axis either along $(100)_{Ge}$ or $(010)_{Ge}$ as was already observed in Refs. 10 and 15.
(2) c-axis either along $(100)_{Ge}$ or $(010)_{Ge}$. A very small component can also be detected with the c-axis along $(110)_{Ge}$ but it is at least 20 times less intense than for the c-axis along $(100)_{Ge}$.

The relative intensities measured for a (002) reflection (for the clusters with a c-axis in-plane) and a (211) (for the c-axis out-of-plane) indicates, after taking into account theoretical intensities from bulk Ge_3Mn_5 that there is $\approx 97\pm1\%$ of the clusters with a c-axis perpendicular to the sample surface. In order to avoid any effect from the sample miscut, the intensities of the (002) and (211) reflections were compared around the same azimuthal angle. The widths of radial scans around (211) reflections indicate that the average cluster size is 10.6 ± 1 nm, and does not depend on the azimuth. The same size is found for the clusters with in-plane c-axis. Moreover, the exact coordinates for the (211) reflections for this main family of clusters showed that their lattice is distorted compared to the bulk hexagonal lattice. A refinement using seven (211) reflections for the clusters with their a-axis parallel to $(010)_{Ge}$, yielded the following in-plane parameters for these clusters: $a=0.7229$ nm, $b=0.7197$ nm, and $\gamma=120.16°$ (as compared to bulk value of 0.7184 nm). This indicates that the clusters are strained due to epitaxial strain by the germanium matrix due to lattice mismatch. Note that even though the majority orientation of Ge_3Mn_5 clusters is similar to that of Ref. 10, their study corresponds to a high-temperature growth rather than *ex situ* annealing. In other results (not shown here), we have found that high-temperature growth increases the fraction of precipitates with their c-axis in-plane.

IV. MAGNETIC PROPERTIES

The magnetic properties of Ge_3Mn_5 clusters were studied using SQUID magnetometry. Figure 3(a) shows the saturation magnetization of Ge_3Mn_5 clusters as a function of temperature. We can clearly observe two different phases: the Ge_3Mn_5 with a Curie temperature of 300 ± 5 K and the paramagnetic contribution of Mn ions in the Ge matrix. After subtracting the signal of Ge_3Mn_5, the signal from diluted Mn ions is obtained and fitted using a Brillouin function. If we assume that Mn atoms are in substitutional position with a magnetic moment of 3 μ_B,[16] we deduce that the Mn concentration in the Ge matrix is of the order of 2% (neglecting the volume fraction of precipitates). This value is in rather good agreement with that obtained by EELS which gives an average Mn content in the Ge matrix between 0% and 1% which is the resolution limit of this technique. Zero field cooled-field cooled (ZFC-FC) measurements as well as the temperature dependence of magnetic remanence show that Ge_3Mn_5 clusters are superparamagnetic with an apparent blocking temperature of $T_B=265\pm5$ K (Fig. 3).

Hysteresis curves at 5 K in Fig. 4 clearly show that most of Ge_3Mn_5 clusters exhibit perpendicular magnetic anisotropy. Since the clusters are spherical, perpendicular anisotropy arises from magnetocrystalline anisotropy. Bulk

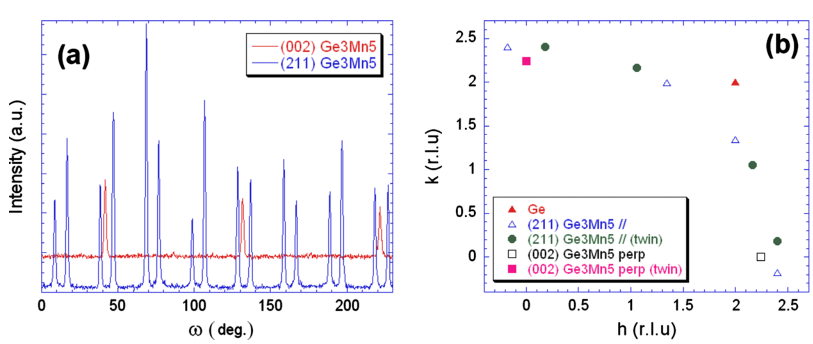

FIG. 2. (Color online) (a) Grazing incidence XRD angular scans performed around the 2θ Bragg angle of the $(002)_{Ge_3Mn_5}$ and $(211)_{Ge_3Mn_5}$ in-plane reflections. Four types of clusters are present, as explained in (b) with the location of all reflections relatively to the Ge lattice: two clusters with their c-axis perpendicular to the Ge surface, and their (100) direction either parallel to $(100)_{Ge}$ or $(010)_{Ge}$, and two with their c-axis either along $(100)_{Ge}$ or $(010)_{Ge}$. Small ($\approx$20%) intensity variations of equivalent reflections with ω in (a) are due to a small miscut in the sample, and also to the in-plane distortion of the Ge_3Mn_5 crystal.

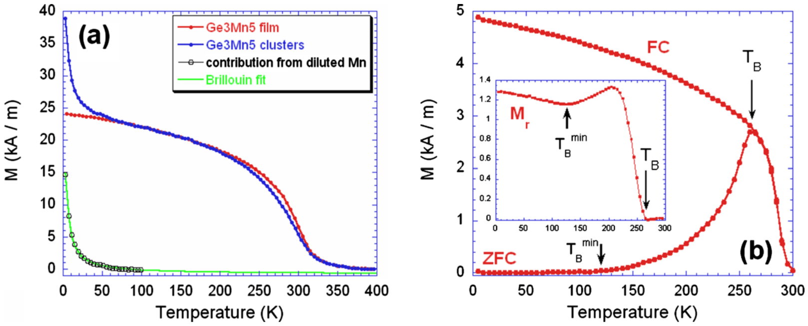

FIG. 3. (Color online) (a) Temperature dependence of the saturation magnetization of a $Ge_{0.94}Mn_{0.06}$ film grown at 130 °C and annealed at 650 °C during 15 min. The applied field is 2 T in the film plane. (b) ZFC-FC measurements performed on a $Ge_{0.94}Mn_{0.06}$ film grown at 100 °C and annealed at 650 °C for 15 min. The magnetic field is applied at 60° with respect to the film plane. Inset: magnetic remanence after maximum field cooling under 5 T.

Ge_3Mn_5 crystal is hexagonal with uniaxial magnetic anisotropy along the c-axis, hence most of Ge_3Mn_5 clusters have their c-axis perpendicular to the film plane in good agreement with XRD data. From hysteresis loops, we can estimate that 70% of the magnetic signal corresponds to these clusters having c-axis perpendicular to the film plane. As shown in the inset of Fig. 4, out-of-plane coercive fields range between 0.2 ± 0.05 T and 0.6 ± 0.05 T. This field dispersion arises from the cluster size distribution as shown in the TEM images of Fig. 1. Indeed for the smallest clusters, magnetization reversal is thermally activated giving the lowest coercive field value: 0.2 ± 0.05 T. On the other hand, for the largest blocked particles, the maximum coercive field gives the anisotropy field $\mu_0 H_{a2} = 0.6 \pm 0.05$ T of a single-domain cluster according to the Stoner and Wohlfarth model.[17] Using the bulk M_S value (1100 kA/m),[18] we deduce the anisotropy constant: $K_2 = \mu_0 H_{a2} M_S / 2 \approx 3.3 \times 10^5$ J/m^3 which is less than the reported bulk value 4.2×10^5 J/m^3.[19] This may be explained by the distortion of Ge_3Mn_5 lattice due to the epitaxial-strain of the (Ge,Mn) matrix as observed in the diffraction. If we assume that undistorted clusters exhibit the bulk anisotropy constant, the effective magnetoelastic anisotropy constant K_{ME} is then simply given by: $K_{ME} = 4.2 \times 10^5 - 3.3 \times 10^5 = 0.9 \times 10^5$ J/m^3. This result shows that magnetic anisotropy in Ge_3Mn_5 is very sensitive to slight crystal distortion. However, further systematic study is required to derive the exact dependence of magnetic anisotropy on crystal distortion. By using the Néel–Brown model:[17] $K_2 V = 25 k_B T_B$ we find the actual blocking temperature of Ge_3Mn_5 clusters of average size 10.6 nm: $T_B = 596.5$ K. This value is much higher than the Curie temperature and thus cannot be measured by ZFC-FC measurements. Moreover the lowest blocking temperature $T_B^{min} \approx 120$ K [see Fig. 3(b)] yields a cluster diameter of ≈6.2 nm which corresponds to a lower bound for the cluster size. If we further assume that the cluster size distribution is Gaussian-like and centered around 10.6 nm, we finally find the maximum cluster diameter: ≈10.6+4.4=15 nm. Hence Ge_3Mn_5 clusters grown by annealing (Ge,Mn) films exhibit a very broad size distribution. In Fig. 4, we observe a magnetic signal with low coercive field which may have different origins: (i) Ge_3Mn_5 clusters with their c-axis in-plane, (ii) Ge_3Mn_5 clusters with in-plane magnetic anisotropy due to oblate shape, or (iii) Mn-rich precipitates that remain despite the high annealing temperature and exhibit a very low coercive field.

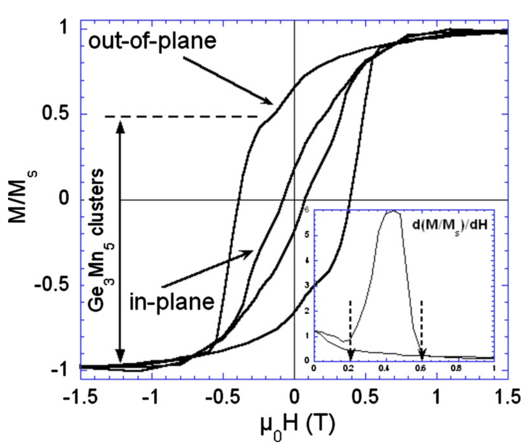

FIG. 4. (Color online) Hysteresis loops recorded at 5 K for the applied field parallel and perpendicular to the film plane. Inset: derivative of M/M_s for out-of-plane positive fields.

Case (i) is unlikely because in XRD we observe only 3 ± 1% of clusters having their c-axis in the film-plane along [100] and [010] directions. This population is not large enough to account for the low coercive field signal. For case (ii), we observe only spherical clusters in HRTEM image which rules out the possibility of having oblate clusters leading to in-plane shape anisotropy. We believe that case (iii) is most likely and the magnetic signal at low coercive field may originate from amorphous Mn-rich precipitates that remain in the film despite annealing at high temperature. This is supported by temperature dependent hysteresis curves (not shown), where the low coercive field signal disappears above 200 K. This temperature is just above the Curie temperature of Mn-rich amorphous (Ge,Mn) phase[20] and this amorphous phase cannot be detected by XRD. The EPR spectra from (Ge,Mn) film containing Ge_3Mn_5 clusters is shown in Fig. 5. We observe ferromagnetic peaks only when external field is applied in the film plane, corresponding to the clusters having out-of-plane anisotropy. These peaks are quite sensitive and disappears rapidly with change in field angle. From Smit-Beljer formalism[21] we obtain the anisotropy field to be 0.42 T as compared to 0.4 T which is the median value obtained from SQUID measurements (see inset in Fig. 4), exhibiting a good correlation between the two techniques.

V. SUMMARY

To summarize, we have grown Ge_3Mn_5 clusters by annealing (Ge,Mn) films grown at low temperature. This procedure leads to very broad size distributions of spherical clusters located away from the surface deep inside the germanium film. 97% of these clusters exhibit strong out-of-

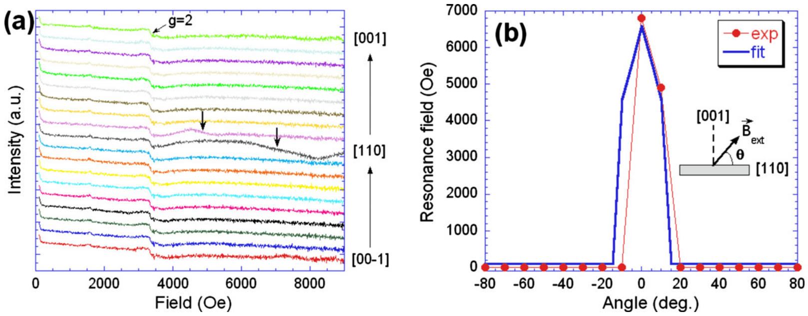

FIG. 5. (Color online) (a) The EPR spectra for X-band (9.4 GHz) of Ge_3Mn_5 clusters at 5 K. (b) Angular dependence of the resonance field. The angle is defined between the film plane and the direction of the applied static magnetic field. The angular step in goniometer during measurement has been 10°.

plane magnetic anisotropy. However perpendicular anisotropy is less than the expected bulk value due to a clear in-plane distortion of the crystal lattice induced by epitaxial strain in the germanium matrix. These Ge_3Mn_5 clusters are thus model systems for the study of hybrid FMS systems. In the future, new growth techniques have to be explored in order to improve the control over the size, location, and magnetic anisotropy of these clusters and use them in vertical heterostructures for spintronic applications.

ACKNOWLEDGMENTS

The authors would like to thank Dr. Joel Cibert for his significant input and the staff from BM02 and BM32 beamlines of the European Synchrotron Radiation Facility (ESRF, Grenoble, France) for providing beamtime. This work was partly supported by the French Agence Nationale pour la Recherche (ANR project GeMO) and the Nanoscience Foundation of Grenoble in France (RTRA project IMAGE).

[1] A. H. MacDonald, P. Schiffer, and N. Samarth, Nature Mater. **4**, 195 (2005).
[2] H. Ohno, Science **281**, 951 (1998).
[3] A. Bonanni and T. Dietl, Chem. Soc. Rev. **39**, 528 (2010).
[4] M. Jamet, A. Barski, T. Devillers, V. Poydenot, R. Dujardin, P. Bayle-Guillemaud, J. Roth-man, E. Bellet-Amalric, A. Marty, and J. Cibert, Nature Mater. **5**, 653 (2006).
[5] S. Kuroda, N. Nishizawa, K. Takita, M. Mitome, Y. Bando, K. Osuch, and T. Dietl, Nature Mater. **6**, 440 (2007).
[6] A. Bonanni, A. Navarro-Quezada, T. Li, M. Wegscheider, R. T. Lechner, G. Bauer, M. Rovezzi, F. D'Acapito, F. Kiecana, M. Sawicki, and T. Dietl, Phys. Rev. Lett. **101**, 135502 (2008).
[7] P. N. Hai, S. Ohya, M. Tanaka, S. E. Barnes, and S. Maekawa, Nature (London) **458**, 489 (2009).
[8] C. Bihler, C. Jaeger, T. Vallaitis, M. Gjukic, M. S. Brandt, E. Pippel, J. Woltersdorf, and U. Gösele, Appl. Phys. Lett. **88**, 112506 (2006).
[9] S. Ahlers, D. Bougeard, N. Sircar, G. Abstreiter, A. Trampert, M. Opel, and R. Gross, Phys. Rev. B **74**, 214411 (2006).
[10] R. T. Lechner, V. Holý, S. Ahlers, D. Bougeard, J. Stangl, A. Trampert, A. Navarro-Quezada, and G. Bauer, Appl. Phys. Lett. **95**, 023102 (2009).
[11] S. Zhou, A. Shalimov, K. Potzger, N. M. Jeutter, C. Baehtz, M. Helm, J. Fassbender, and H. Schmidt, Appl. Phys. Lett. **95**, 192505 (2009).
[12] T. Devillers, M. Jamet, A. Barski, V. Poydenot, P. Bayle-Guillemaud, E. Bellet-Amalric, S. Cherifi, and J. Cibert, Phys. Rev. B **76**, 205306 (2007).
[13] O. Kazakova, R. Morgunov, J. Kulkarni, J. Holmes, and L. Ottaviano, Phys. Rev. B **77**, 235317 (2008).
[14] R. Morgunov, M. Farle, M. Passacantando, L. Ottaviano, and O. Kazakova, Phys. Rev. B **78**, 045206 (2008).
[15] V. Holý, R. T. Lechner, S. Ahlers, L. Horák, T. H. Metzger, A. Navarro-Quezada, A. Trampert, D. Bougeard, and G. Bauer, Phys. Rev. B **78**, 144401 (2008).
[16] T. C. Schulthess and W. H. Butler, J. Appl. Phys. **89**, 7021 (2001).
[17] M. Jamet, W. Wernsdorfer, C. Thirion D. Mailly, V. Dupuis, P. Mélinon, and A. Pérez, Phys. Rev. Lett. **86**, 4676 (2001).
[18] J. B. Forsyth and P. J. Brown, J. Phys.: Condens. Matter **2**, 2713 (1990).
[19] Y. Tawara and K. Sato, J. Phys. Soc. Jpn. **18**, 773 (1963).
[20] S. Sugahara, K. L. Lee, S. Yada, and M. Tanaka, Jpn. J. Appl. Phys., Part 2 **44**, L1426 (2005).
[21] J. Smit and H. G. Beljers, Philips Res. Rep. **10**, 113 (1955).